

Binding of Alkenes to ReS_4^-

Jonathan T. Goodman and Thomas B. Rauchfuss*

Contribution from the School of Chemical Sciences, University of Illinois, Urbana, Illinois 61801

Received December 18, 1998

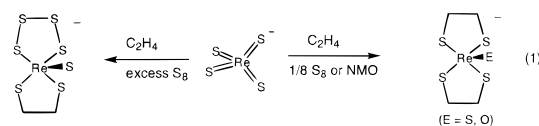
Abstract: The tetrathioperrhenate anion, ReS_4^- (**1**), is shown to form adducts with a variety of alkenes. The alkene adducts form reversibly, and those of norbornene and norbornadiene were isolated. For norbornene, the K_{eq} 's range from 12 000 (CH_2Cl_2 solution) to 2650 M^{-1} (pyridine solution). The following values were determined (MeCN soln): $\Delta H = -53 \text{ kJ mol}^{-1}$ and $\Delta S = -98 \text{ J mol}^{-1} \cdot \text{K}^{-1}$. The solid-state structures of adducts derived from norbornene and norbornadiene, $\text{Ph}_4\text{P}[\text{ReS}_2(\text{S}_2\text{C}_7\text{H}_{10})]$ (**2**) and $(\text{Ph}_4\text{P})_2[(\text{ReS}_2)_2(\text{S}_4\text{C}_7\text{H}_8)]$, respectively, reveal tetrahedral Re centers wherein the Re–SR bonds are elongated by 0.1 Å compared to those in **1**. Additionally, the RS–Re–SR angle is contracted to 86.7°, reflecting the constraint of the chelate backbone. Electrochemical measurements show that the reduction of **2** induces dissociation of norbornene from ReS_4^{2-} . Ethylene binds to **1** only weakly at room temperature, but this adduct is directly observable by low-temperature UV/vis spectroscopy. The adduct of dimethyl maleate and **1** could only be observed in the neat alkene; **1** does not catalyze the isomerization of dimethyl maleate to dimethyl fumarate.

Introduction

A variety of metal oxides, including MnO_4^- , RuO_4 , and OsO_4 are useful oxygen-atom transfer agents.^{1–4} Due to its catalytic activity, OsO_4 has been examined particularly intensely. Recent experimental studies have focused on the asymmetric dihydroxylation process,^{5–9} while theoretical studies have dealt with the initial mode of alkene binding to OsO_4 .^{10–14} Many variations on OsO_4 have been examined including the related Ru^{VII} reagents,^{4,15,16} ligand-modified (asymmetric) catalysts,^{17–19} and the corresponding imido-oxides $\text{OsO}_3(\text{NR})$.^{20–22} In principle,

isoelectronic metal sulfides could be used to effect the corresponding addition of sulfur across the double bond of alkenes.^{23–25} Aside from synthetic implications, this alkene sulfidation reaction would contribute new insights into the energetics and mechanism of the oxidation process. It is also reasonable to expect that such sulfidation reactions would shed light on the organic chemistry of metal sulfides, which is highly relevant to the hydrodesulfurization process.²⁶

An obvious approach to alkene sulfidation would involve the use of the sulfido analogue of OsO_4 , i.e., OsS_4 , but this compound is unknown. We predict that OsS_4 would not be stable, although Shapley et al. have prepared a complex with a terminal sulfido ligand.²⁷ ReS_4^- is isoelectronic with OsO_4 , and as we show in this paper, it reacts with alkenes.^{28,29} These findings are relevant to a previous report that, in the presence of oxidants, ReS_4^- reacts with alkenes to produce bis(alkanedithiolato)Re(V) complexes (eq 1).³⁰



This transformation is analogous to one invoked in the chemistry of OsO_4 .^{6,7} The bis(alkanedithiolato) complex obviously arise

- (1) Holm, R. H.; Donahue, J. P. *Polyhedron* **1993**, *12*, 571–589.
- (2) Holm, R. H. *Chem. Rev.* **1987**, *87*, 1401–1449.
- (3) Fatiadi, A. J. *Synthesis* **1987**, 85–127.
- (4) Ley, S. V.; Norman, J.; Griffith, W. P.; Marsden, S. P. *Synthesis (Stuttgart)* **1994**, *7*, 639–666.
- (5) Gobel, T.; Sharpless, K. B. *Angew. Chem., Int. Ed. Engl.* **1993**, *32*, 1329–1331.
- (6) Wai, J. S. M.; Marko, I.; Svendsen, J. S.; Finn, M. G.; Jacobsen, E. N.; Sharpless, K. B. *J. Am. Chem. Soc.* **1989**, *111*, 1123–1125.
- (7) Kwong, H.-L.; Sorato, C.; Ogino, Y.; Chen, H.; Sharpless, K. B. *Tetrahedron Lett.* **1990**, *31*, 2999–3002.
- (8) Corey, E. J.; Xu, F.; Noe, M. C. *J. Am. Chem. Soc.* **1997**, *119*, 12414–12415.
- (9) Corey, E. J.; Sarshar, S.; Azimioara, M. D.; Newbold, R. C.; Noe, M. C. *J. Am. Chem. Soc.* **1996**, *118*, 7851–7852.
- (10) Dapprich, S.; Ujaque, G.; Maseras, F.; Lledos, A.; Musaev, D. G.; Morokuma, K. *J. Am. Chem. Soc.* **1996**, *118*, 11660–11661.
- (11) Torrent, M.; Deng, L.; Duran, M.; Sola, M.; Ziegler, T. *Organometallics* **1997**, *16*, 13–19.
- (12) Jorgensen, K. A. *Tetrahedron Lett.* **1990**, *31*, 6417.
- (13) Veldkamp, A.; Frenking, G. *J. Am. Chem. Soc.* **1994**, *116*, 4937–4946.
- (14) Becker, H.; Sharpless, K. B. *Angew. Chem., Int. Ed. Engl.* **1996**, *35*, 448–451.
- (15) Norrby, P. O.; Kolb, H. C.; Sharpless, K. B. *Organometallics* **1994**, *13*, 344–347.
- (16) Ley, S. V.; Bolli, M. H.; Hinzen, B.; Gervois, A. G.; Hall, B. J. *J. Chem. Soc., Perkin Trans. 1* **1998**, 2239–2241.
- (17) Kolb, H. C.; Vannieuwenhze, M. S.; Sharpless, K. B. *Chem. Rev.* **1994**, *94*, 2483–2547.
- (18) Berrisford, D. J.; Bolm, C.; Sharpless, K. B. *Angew. Chem., Int. Ed. Engl.* **1995**, *34*, 1059–1070.
- (19) Criegee, R. *Justus Liebigs Ann. Chem.* **1936**, 75–96.
- (20) Bruncko, M.; Schlingloff, G.; Sharpless, K. B. *Angew. Chem., Int. Ed. Engl.* **1997**, *36*, 1483–1486.
- (21) Li, G.; Chang, H. T.; Sharpless, K. B. *Angew. Chem., Int. Ed. Engl.* **1996**, *35*, 451–454.

- (22) Li, G.; Sharpless, K. B. *Acta Chem. Scand.* **1996**, *50*, 649–651.
- (23) Rakowski DuBois, M.; Jagirdar, B.; Noll, B.; Dietz, S. *Transition Metal Sulfur Chemistry*; Stiefel, E. I., Matsumoto, K., Eds.; ACS Symposium Series 653; American Chemical Society: Washington, DC, 1996.
- (24) Koval, C. R.; Lopez, L. L.; Kaul, B. B.; Renshaw, S.; Green, K.; Rakowski DuBois, M. *Organometallics* **1995**, *14*, 3440–3447.
- (25) Rakowski DuBois, M. *Chem. Rev.* **1989**, *89*, 1–9.
- (26) Topsøe, H.; Clausen, B. S.; Massoth, F. E. *Hydrotreating Catalysis, Science and Technology*; Springer-Verlag: Berlin, 1996.
- (27) Shapley, P. A.; Liang, H. C.; Shusta, J. M.; Schwab, J. J.; Zhang, N. J.; Wilson, S. R. *Organometallics* **1994**, *13*, 3351–3359.
- (28) Wei, L.; Halbert, T. R.; Murray, H. H., III; Stiefel, E. I. *J. Am. Chem. Soc.* **1990**, *112*, 6431.
- (29) Murray, H. H.; Wei, L. W.; Sherman, S. E.; Greaney, M. A.; Eriksen, K. A.; Carstensen, B.; Halbert, T. R.; Stiefel, E. I. *Inorg. Chem.* **1995**, *34*, 841–853.
- (30) Goodman, J. T.; Inomata, S.; Rauchfuss, T. B. *J. Am. Chem. Soc.* **1996**, *118*, 11674.

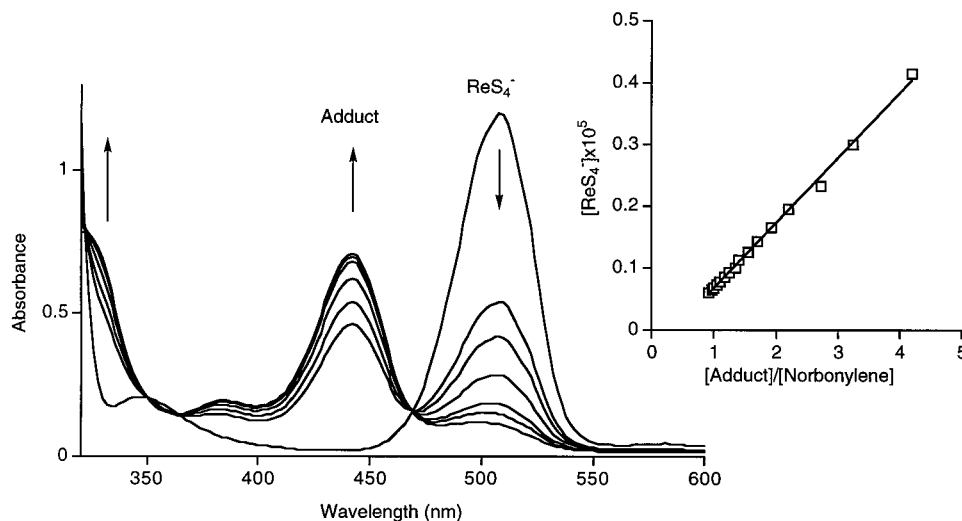


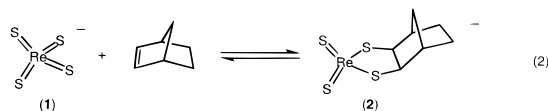
Figure 1. Optical spectra of a MeCN solution of $(\text{Et}_4\text{N})\mathbf{1}$ (9.4×10^{-5} M) upon titration with a 0.056 M solution of norbornene. Plot of $[\mathbf{1}]$ vs $[\mathbf{2}]/[\text{C}_7\text{H}_{10}]$ in MeCN (slope = $1/K_{\text{eq}}$; $K_{\text{eq}} = 9400 \text{ M}^{-1}$).

via a multistep process, probably involving the initial addition of the alkene to **1**. In this report we focus on this simple reaction, the addition of alkenes to ReS_4^- .

Results and Discussion

ReS_4^- reversibly binds alkenes with affinities that vary with the substituents on the organic substrate. The paragraphs below focus primarily on the stable adducts derived from norbornene and related strained olefins. Subsequent sections survey the reactions of **1** with other alkenes.

Norbornene + ReS_4^- . It is well-known that norbornenes (2.2.1-bicycloheptenes) undergo cycloaddition reactions more readily than most alkenes, due to the thermodynamic benefits of the release of ring strain.³¹ The optical spectrum of a solution of **1** and norbornene reveals a new absorption at 442 nm in addition to the 508 nm band characteristic of ReS_4^- . All alkene adducts examined in this study have a band near 440 nm (see below). Dilution of norbornene:**1** solutions result in the decrease of the absorbance at 442 nm and a corresponding increase of the 508 nm band (eq 2).



Isobestic behavior was observed upon the incremental addition of norbornene to a solution of **1** (Figure 1). Plots of $[\text{ReS}_4^-]$ vs $[\text{adduct}]/[\text{norbornene}]$ were linear with a slope of K_{eq}^{-1} (Figure 1). For the reaction depicted in eq 1, the K_{eq} is $\sim 9400 \text{ M}^{-1}$ (23 °C, CH_3CN solution).³² The K_{eq} displayed a measurable solvent dependence but does not correlate with dielectric constant (indicated in parentheses): $K_{\text{eq}} = 12\,000$ (CH_2Cl_2 , 8.93), 9400 (CH_3CN , 36.64), 5000 ($(\text{EtO})_3\text{PO}$: 13.2), 2650 M^{-1} (pyridine: 13.2). At 296 K, the $\sim 4\times$ change in K_{eq} (CH_2Cl_2 vs pyridine) corresponds to a $\Delta\Delta G = 3.7 \text{ kJ mol}^{-1}$.

To determine the thermodynamic parameters associated with eq 2, we evaluated K_{eq} over the range 5–50 °C ($[\text{ReS}_4^-]_0 = 2.16 \times 10^{-4} \text{ M}$, $[\text{C}_7\text{H}_{10}]_0 = 1.13 \times 10^{-4} \text{ M}$). The equilibrium constant was deduced from changes in the absorbance (A), i.e., $A[\text{ReS}_4^-]_0$ vs $A[\text{ReS}_4^-]$ (Figure 2). The relative concentration

of the adduct increased at lower temperatures, indicative of an exothermic process. Plots of $\ln(K_{\text{eq}})$ vs T^{-1} were linear, yielding the following values: $\Delta H = -53 \text{ kJ mol}^{-1}$ and $\Delta S = -98 \text{ J}\cdot\text{mol}^{-1}\cdot\text{K}^{-1}$ (Figure 2).

The strong binding of norbornene to **1** allowed us to isolate the adduct, $\text{Ph}_4\text{P}[\text{ReS}_2(\text{S}_2\text{C}_7\text{H}_{10})]$ ($\text{Ph}_4\text{P}[\mathbf{2}]$) in analytically pure form. The gold-colored crystals are air stable, although the solutions are not. The ^1H NMR data for **2** is straightforward: the major changes in the chemical shifts relative to free norbornene are associated with the olefinic and bridgehead protons. These resonances shift from δ 5.99 and 2.82 to δ 2.31 and 2.47, respectively. The IR spectrum of **2** consists of a pair of intense bands near 500 cm^{-1} ; these are assigned as $\nu_{(\text{ReS}_2)_{\text{sym}}}$ and $\nu_{(\text{ReS}_2)_{\text{asym}}}$. In contrast, ν_{ReS} for **1** is 488 cm^{-1} .³³

The binding of norbornene to **1** was also studied by dynamic ^1H NMR spectroscopy. Given the large formation constant of the adduct, the exchange process is limited by the rate of alkene dissociation. The ^1H NMR spectrum of **2** is invariant over the range -20 – 60 °C, both in the presence and absence of free norbornene. The signals of interest are those for the alkene and the corresponding *ipso* CH's of the thiolate (the adduct **2**); these signals are separated by 3.7 ppm, which, for a 500 MHz spectrometer, corresponds to an off rate of $\sim 2000 \text{ s}^{-1}$. Clearly, the dissociation rate process is significantly slower than this value. In an attempt to directly observe this slower rate process we employed the magnetization transfer technique in which we irradiated the alkenyl signals for norbornene and observed the effects on the thiolate *ipso* signals. The T_1 for these *ipso* signals (7 s) allows us to measure rates down to $\sim 0.14 \text{ s}^{-1}$ ($\sim 1/T_1$). At long saturation times (20 °C), these thiolate signals decreased to $\sim 25\%$ of their original intensity, indicating that the alkene dissociates at rates comparable to $1/T_1$.

Electrochemical Studies. The cyclic voltammogram (CV) for **2** provides further insight into the binding of the alkene (all potentials are referenced to Ag/AgCl). Of particular interest is the fact that the CV (Figure 3) of **2** (MeCN solution) showed an irreversible reduction at -1.72 V , $\sim 450 \text{ mV}$ more reducing than the ReS_4^{2-} couple. Beyond the $\text{ReS}_2(\text{S}_2\text{C}_7\text{H}_{10})^{2-}$ couple, we observed a reversible reduction wave at -2.06 V , which, as we verified, is due to the $\text{ReS}_4^{2-/3-}$ couple.³³ When the direction of the CV sweep was reversed, we observed oxidations

(31) Brown, H. C.; Kawakami, J. H.; Liu, K.-T. *J. Am. Chem. Soc.* **1973**, *95*, 2209–2216.

(32) Parker, A. J. *Chem. Rev.* **1969**, *69*, 1–32.

(33) Do, Y.; Simhon, E. D.; Holm, R. H. *Inorg. Chem.* **1985**, *24*, 4635–4642.

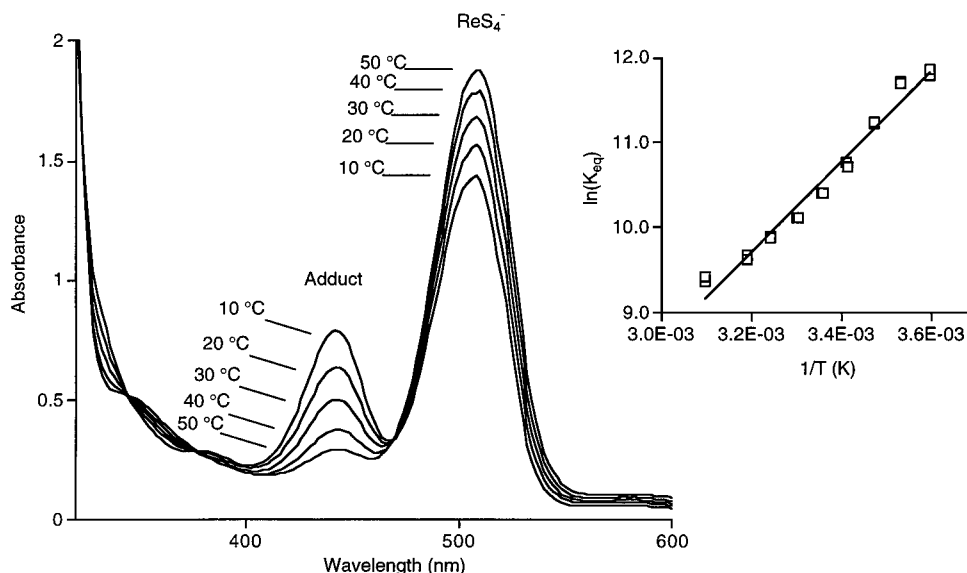


Figure 2. Dependence of K_{eq} (see eq 2) vs T . A van't Hoff plot for the equilibrium **1** + norbornene.

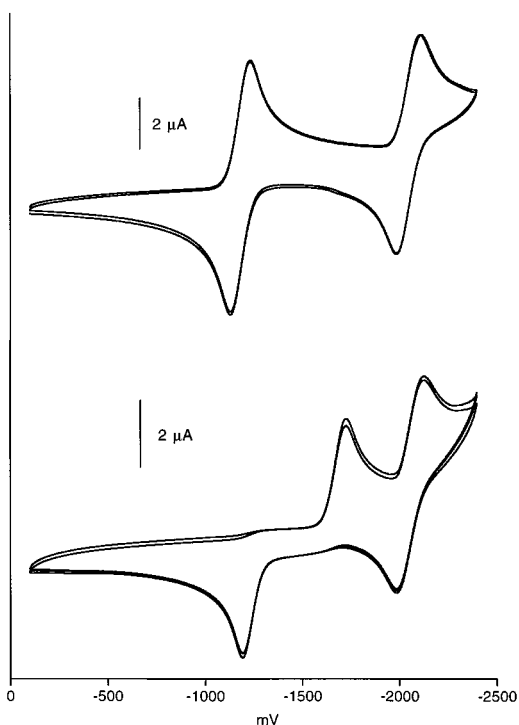
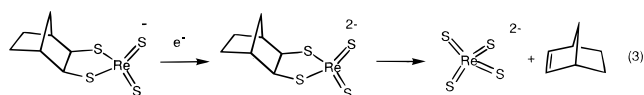


Figure 3. Cyclic voltammogram of 10^{-3} M MeCN solutions (10^{-1} M Bu_4NPF_6) of $\text{Et}_4\text{N1}$ and $\text{Et}_4\text{N2}$ (potentials vs Ag/AgCl), sweep rate = 400 mV/s.

corresponding to $\text{ReS}_4^{3-/2-}$ (-2.06 V) and $\text{ReS}_4^{2-/1-}$ (-1.25 V), again as seen in solutions of **1**. Overall, the reductive processes for **2** indicate an electrochemical–chemical (E–C) process whereby reduction of **2** to $\text{ReS}_2(\text{S}_2\text{C}_7\text{H}_{10})^{2-}$ induces the dissociation of norbornene from ReS_4^{2-} (eq 3).³⁴



Furthermore the potential for the couple $\text{ReS}_2(\text{S}_2\text{C}_7\text{H}_{10})^{-/2-}$, vs $\text{ReS}_4^{-/2-}$ is consistent with the description of **2** as a Re(V) complex.

Binding of Norbornene to Solid Samples of 1. The uptake of norbornene vapor by powdered samples of **1** is signaled by conversion of the purple-black solid to yellow. Qualitatively, the rate of gas sorption varies with the crystallinity of the samples. When loaded on basic alumina ($\sim 5\%$ mass loading), the sorption process is more rapid: $\mathbf{1} \cdot \text{Al}_2\text{O}_3$ rapidly reacts with norbornene vapor, indicated by a rapid change of color from violet to yellow along the vapor pathway. The change in mass of the $\mathbf{1} \cdot \text{Al}_2\text{O}_3$, upon exposure to norbornene, although imprecisely determined, is consistent with the binding of one alkene to **1**. The addition of norbornene to solid samples of **1** is also apparent in the IR spectrum. The absorption at 488 cm^{-1} for **1** is replaced by absorptions at 500 and 415 cm^{-1} upon addition of norbornene. The loss of norbornene from microcrystalline samples of **2** was monitored by thermogravimetric analysis (TGA). At $161 \text{ }^\circ\text{C}$ solid samples of **2** rapidly lose 10.5% of their mass (theory: 12.5%).

Other Strained Alkenes + ReS_4^- . Dicyclopentadiene, which features one norbornene-like alkene subunit, binds to **1** to give a stable adduct. The optical spectra of this adduct and **2** are nearly identical. We therefore assume that these compounds are structurally analogous. The equilibrium constant, K_{eq} ($23 \text{ }^\circ\text{C}$, MeCN), for the binding of dicyclopentadiene to ReS_4^- was $\sim 2500 \text{ M}^{-1}$.

The reaction of **1** and an excess of norbornadiene gave $[\text{ReS}_2(\text{S}_2\text{C}_7\text{H}_8)]^-$ in high yield. The ^1H NMR spectrum of this adduct showed well-separated signals for the bound and free alkene hydrogen atoms. The corresponding 2:1 adduct, $[(\text{ReS}_2)_2(\text{S}_4\text{C}_7\text{H}_8)]^{2-}$, could be prepared by treatment of **1** with 0.5 equiv of norbornadiene. The IR and UV/vis spectra of this 2:1 adduct are nearly identical to those for **2**, while the ^1H NMR spectrum is consistent with a symmetrical structure.

Solid State Structure of Norbornene and Norbornadiene Adducts. Single crystals of $\text{Ph}_4\text{P}[\mathbf{2}]$ and the 2:1 adduct of norbornadiene were examined by single crystal X-ray diffraction (Figures 4 and 5). In both cases, the geometries about the Re centers are very similar. The Re atom is tetrahedrally coordinated to two terminal and two thiolato sulfur atoms. The stereochemistry of the dithiolate confirms exo addition of the norbornene to **1**. Other complexes of norbornanedithiolate have been prepared from the preformed dithiol.^{35–37} The Re coord-

(34) Bard, A. J.; Faulkner, L. R. *Electrochemical Methods Fundamentals and Applications*; J. Wiley: New York, 1980.

(35) See: Stephan, D. W.; Nadasdi, T. T. *Coord. Chem. Rev.* **1996**, *147*, 147–208.

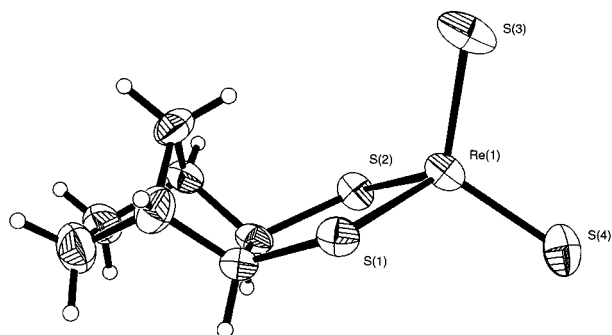


Figure 4. Structure of the anion in $(\text{Ph}_4\text{P})_2$ with thermal ellipsoids at 50% probability level.

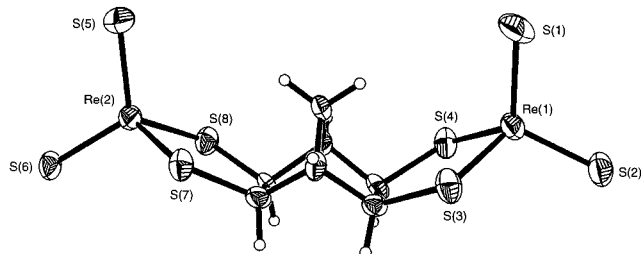


Figure 5. Structure of the dianion in $(\text{Ph}_4\text{P})_2[(\text{ReS}_2)_2\text{S}_4\text{C}_7\text{H}_8]$ with thermal ellipsoids at 50% probability level.

Table 1. Selected Bond Distances (Å) and Angles (deg) for $\text{Ph}_4\text{P}[\text{ReS}_2(\text{S}_2\text{C}_7\text{H}_{10})]$ and $(\text{Ph}_4\text{P})_2[(\text{ReS}_2)_2(\text{S}_4\text{C}_7\text{H}_8)]$

$\text{Ph}_4\text{P}[\text{ReS}_2(\text{S}_2\text{C}_7\text{H}_{10})]$		$(\text{Ph}_4\text{P})_2[(\text{ReS}_2)_2(\text{S}_4\text{C}_7\text{H}_8)]$	
Re1-S4	2.1267(11)	Re1-S1	2.117(4)
Re1-S3	2.1320(13)	Re1-S2	2.131(4)
Re1-S2	2.2277(11)	Re2-S5	2.134(4)
Re1-S1	2.2280(11)	Re2-S6	2.127(3)
		Re1-S3	2.230(4)
		Re1-S4	2.223(4)
		Re2-S7	2.234(4)
		Re2-S8	2.218(3)
S1-Re1-S2	86.70(4)	S3-Re1-S4	86.72(13)
		S7-Re2-S8	86.93(12)

dination environment is only slightly distorted from that in **1**. The bond distances from Re to the terminal sulfides are essentially unchanged, while the distance from Re to the thiolato sulfur atoms have increased by ~ 0.1 Å (Table 1). Whereas the S-Re-S angle is 109.5° in **1**, the RS-Re-SR angle is 86.7° in **2**, reflecting the constraints of the chelating organosulfur ligand. In both adducts, the ReS_4^- moieties have added exo with respect to the norbornene unit, as has been observed for norbornanediolato complexes.³⁸

Ethylene and Dimethyl Maleate. Ethylene (1 atm) does not form a room-temperature-stable adduct with **1**. A 0.14 mM solution of **1** in MeCN shows less than a 5% decrease in the absorbance at 508 nm upon saturation with C_2H_4 at 25°C . Concomitant with this small decrease, a weak band at 442 nm appears. This binding can be easily measured by UV/vis spectroscopy at lower temperatures. The 508 nm absorption, due to free **1**, decreases with decreasing temperature with a corresponding increase in the 440 nm band (Figure 6). The temperature dependence of the shift in the equilibrium ratio is attributed to both the solubility of C_2H_4 and the effect of the

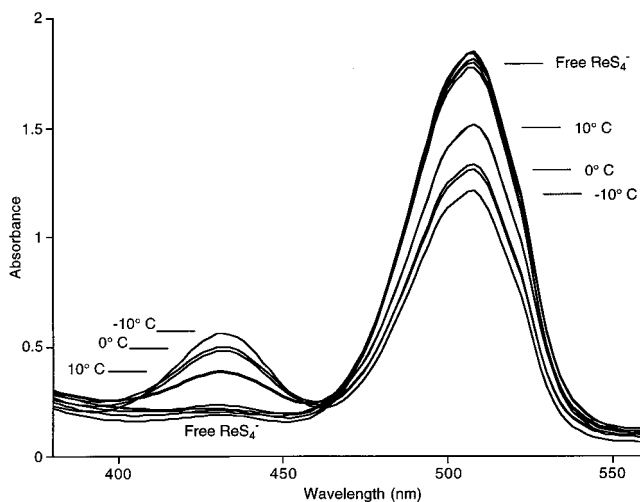


Figure 6. Optical spectrum of Et_4NI (0.14 mM) upon the addition and removal of C_2H_4 at various temperatures.

negative ΔH_{rxn} (see data for norbornene above). When these C_2H_4 -saturated solutions of **1** were purged with N_2 , the recovery of the signal due to **1** was nearly quantitative.

The ^1H NMR spectrum of MeCN solutions of **1** and C_2H_4 showed a weak resonance at δ 2.04, vs 5.40 for dissolved C_2H_4 . Assignment of the δ 2.04 signal to $\text{C}_2\text{H}_4\text{S}_2\text{ReS}_2^-$ was confirmed by magnetization transfer experiments, in which saturation of the δ 5.40 signal decreased the intensity of the δ 2.04 signal.

The addition of dimethyl maleate (>100 equiv) resulted in no measurable effect on the optical properties of the MeCN solutions of **1**. Evidence for adduct formation was observed by dissolving **1** in *neat* dimethyl maleate. Assuming that the extinction coefficient for this adduct and that for **2** are the same, then the ratio $[\text{adduct}]/[\text{ReS}_4^-][\text{dimethyl maleate}]$ indicates $K_{\text{eq}} = 0.3 \text{ M}^{-1}$. ^1H NMR studies show that in the presence of **1**, dimethyl maleate (110°C , 72 h) does not isomerize. This finding indicates that the addition of alkene to ReS_4^- does not proceed through dipolar intermediates, which would otherwise be expected to isomerize the dimethyl maleate to give the thermodynamically favored *trans*-alkene dimethyl fumarate.³⁹

Summary

Stable alkene adducts of ReS_4^- with the strained alkene norbornene and its analogues have been isolated. These stable adducts have spectroscopic characteristics similar to those of less stable derivatives such as those derived from ethylene and dimethyl maleate. Thus, the conclusions drawn from the norbornene derivative are relevant to other alkene adducts. The reactions are well-behaved in the sense that they are cleanly reversible and that single adducts are generated. The reversible binding of alkene is unusual for an inorganic complex, especially where the alkene is not bound to the metal directly, but to an inorganic ligand. The fact that ReS_4^- binds alkenes but ReO_4^- does not suggests that $\text{ReS}_{4-x}\text{Se}_x^-$, no member of which is presently known, will display still greater reactivity. Another Re chalcogenide complex that binds alkenes, Cp^*ReO_3 , forms a stable adduct with norbornene but not with other alkenes.^{38,40} The thermodynamics of the $\text{ReS}_4^-/\text{norbornene}$ and $\text{Cp}^*\text{ReO}_3/\text{norbornene}$ ⁴⁰ reactions are comparable both in terms of ΔH and ΔS . The d^0 -trioxo complex $\text{TcO}_3(\text{bipy})\text{Cl}$ also binds

(36) Tatsumi, K.; Matsubara, I.; Inoue, Y.; Nakamura, A.; Miki, K.; Kasai, N. *J. Am. Chem. Soc.* **1989**, *111*, 7766–7777.

(37) Fox, S.; Wang, Y.; Silver, A.; Millar, M. *J. Am. Chem. Soc.* **1990**, *112*, 3218–3220.

(38) Gable, K. P. *Adv. Organomet. Chem.* **1997**, *41*, 127–161.

(39) Patai, S.; Rappoport, Z. *The Chemistry of Alkenes*; Patai, S., Rappoport, Z., Eds.; Wiley: London, 1964.

(40) Gable, K. P.; Juliette, J. J. *J. Am. Chem. Soc.* **1995**, *117*, 955–962.

styrenes, while the Re analogue does not.⁴¹ As mentioned in the Introduction, unsaturated organic compounds add to organometallic sulfides, e.g., $\text{Cp}^*\text{TiS}^{42}$ and $\text{Cp}_2\text{Mo}_2\text{S}_2(\text{S}_2\text{CH}_2)$.²³

The electrochemical studies provide a rare example of reductively induced dissociation of an alkene adduct. It is interesting to contrast this finding with the results on conventional metal–alkene complexes, which are labilized upon redox. Examples include $\text{Os}(\text{NH}_3)_5(\text{C}_2\text{H}_4)^{2+/3+}$ and related Ru complexes, both of which are labilized upon oxidation.⁴⁴ The fact that ReS_4^{2-} has a lower affinity for alkenes than does ReS_4^- , suggests that alkene binding to **1** is reductive in character. This conclusion is also supported by the fact that the reduction of **2** is ~ 450 mV more forcing than the reduction of **1**. It is well-known that reduction lessens the atom transfer power of metal oxides, as illustrated by the differing reactivity of RuO_4^- and RuO_4 .^{4,35} Other examples of reductively induced scission of $\text{MS}-\text{C}$ bonds exist. Most, but not all, involve fragmentation of coordinated thioethers to generate thiolates.^{35,45–49}

Our results provide clear evidence that inorganic sulfides are fully capable of binding alkenes. The reactivity of **1** with alkenes is also obviously analogous to that seen for OsO_4 . This parallel suggests that the reactivity of other organometallic sulfides may be usefully discussed in the context of the corresponding oxides, a theme also developed in the work of Bergman et al.⁵⁰ In some ways the behavior of **1** suggests commonalities with the inorganic solids of nominal composition Re_2S_7 and MoS_2 , which are widely employed in catalysis.^{26,51,52}

Experimental Section

Reagents and Solvents. All reactions were carried out under a nitrogen atmosphere using standard Schlenk techniques. Except as noted, all reagents are commercially available and were purified prior to use. $\text{NEt}_4[\text{ReS}_4]$ was synthesized using a published procedure.⁵³ $\text{PPh}_4[\text{ReS}_4]$ was prepared by metathesis of $\text{NEt}_4[\text{ReS}_4]$ with PPh_4Br in MeCN solution.

Spectroscopy and Analysis. Microanalyses and thermogravimetry were performed by the School of Chemical Sciences Microanalytical Laboratory. ^1H NMR spectra were recorded on a Varian Unity 500 FT-NMR spectrometer operating at 499.70 MHz. Infrared spectra were obtained on a Mattson Galaxy Series FT-IR 3000 on pressed KBr pellets. UV–vis spectra were obtained on a Hewlett-Packard 8452A diode array spectrophotometer equipped with a constant-temperature bath.

(41) Pearlstein, R. M.; Davison, A. *Polyhedron* **1988**, *7*, 1981–1989.

(42) Sweeney, Z. K.; Polse, J. L.; Andersen, R. A.; Bergman, R. G.; Kubinec, M. G. *J. Am. Chem. Soc.* **1997**, *119*, 4543–4544. Carney, M. J.; Walsh, P. J.; Hollander, F. J.; Bergman, R. G. *Organometallics* **1992**, *11*, 761–777.

(43) For leading references, see: Bennett, M. A.; Heath, G. A.; Hockless, D. C. R.; Kovacok, I.; Willis, A. C. *J. Am. Chem. Soc.* **1998**, *120*, 932–941.

(44) Naota, T.; Takaya, H.; Murahashi, S.-I. *Chem. Rev.* **1998**, *98*, 2599–2660.

(45) Ibrahim, S. K.; Pickett, C. J. *J. Chem. Soc., Chem. Commun.* **1991**, 246–249. Sellmann, D.; Grasser, F.; Knoch, F.; Moll, M. *Angew. Chem., Int. Ed. Engl.* **1991**, *30*, 1311–1312.

(46) Mullen, G. E. D.; Went, M. J.; Wocadlo, S.; Powell, A. K.; Blower, P. *J. Angew. Chem., Int. Ed. Engl.* **1997**, *36*, 1205–1207.

(47) Cha, M. Y.; Shoner, S. C.; Kovacs, J. A. *Inorg. Chem.* **1993**, *32*, 1860–1863.

(48) Abasq, M.-L.; Pétilion, F. Y.; Schollhammer, P.; Talarmin, J. *New J. Chem.* **1996**, *20*, 1221–1233.

(49) Luo, S.; Rauchfuss, T. B.; Gan, Z. *J. Am. Chem. Soc.* **1993**, *115*, 4943.

(50) Sweeney, Z. K.; Polse, J. L.; Andersen, R. A.; Bergman, R. G. *J. Am. Chem. Soc.* **1998**, *120*, 7825–7834.

(51) Weisser, O.; Landa, S. *Sulphide Catalysts, Their Properties, and Applications*; Pergamon: New York, 1973.

(52) Daage, M. *Bulk Metal Sulfides*; Butterworth-Heinemann: New York, 1992.

(53) Exxon Research and Engineering Co. *Synthesis of Tetrathioetherate*. U.S. Patent 88-202342, 1990.

$\text{Ph}_4\text{P}[\text{ReS}_2(\text{S}_2\text{C}_7\text{H}_{10})]$ (**$\text{Ph}_4\text{P}[\mathbf{2}]$).** A 100-mL Schlenk flask was charged with 0.31 g (0.45 mmol) of $\text{Ph}_4\text{P}[\text{ReS}_4]$ and 0.5 g (5.3 mmol) of norbornene followed by 10 mL of CH_3CN . After 10 min, the resulting yellow solution was cooled to ~ -20 °C in a $\text{CO}_2(\text{s})$ /ethylene glycol bath, and dark golden crystals precipitated. A solution of 0.5 g (5.3 mmol) of norbornene in 50 mL of Et_2O was then added over the course of 1 h to the reaction mixture to further precipitate the product. Solvent was decanted from the product, which was washed with 10 mL of Et_2O at -20 °C. The crystals were dried in vacuo. Yield: 0.29 g (85%). Anal. Calcd (found) for $\text{C}_{31}\text{H}_{30}\text{PReS}_4$: C, 49.78 (49.78); H, 4.04 (4.05); P, 4.14 (4.16); Re, 24.89 (24.66); S, 17.15 (17.26). ^1H NMR (500 MHz, CD_3CN) δ 0.607 (1H, ddp, $J = 27, 10, 1.5$ Hz, *apex*), 1.541 (2H, m, *endo*), 1.643 (2H, m, *exo*), 2.310 (2H, d, $J = 1.5$ Hz, *SCH*), 2.476 (1H, dt, $J = 4, 1.5$ Hz, *bridge head*). IR (KBr) 501 and 414 ($\nu_{\text{Re}=\text{S}}$). UV–vis (MeCN soln, with > 10 equiv of norbornene) 442 nm ($\epsilon \sim 7000$ $\text{M}^{-1}\text{cm}^{-1}$).

$\text{Ph}_4\text{P}[\text{ReS}_2(\text{S}_2\text{C}_7\text{H}_8)]$. To a 100-mL Schlenk flask containing a solution of 0.41 g (0.62 mmol) of $\text{Ph}_4\text{P}[\text{ReS}_4]$ in 50 mL of CH_3CN was added 0.067 mL (0.62 mmol) of 2,5-norbornadiene. After 3 h, the reaction solution was concentrated to ~ 10 mL and diluted with 50 mL of Et_2O to precipitate the product. After the solvent was decanted from the solid product, the gold-colored microcrystals were washed with Et_2O , and dried in vacuo. Yield: 0.43 g (94%). Anal. Calcd (found) for $\text{C}_{31}\text{H}_{28}\text{PReS}_4$: C, 49.91 (50.01, 50.09); H, 3.78 (3.69, 3.78); P, 4.15 (3.97); Re, 24.96 (24.63); S, 17.19 (17.45). ^1H NMR (500 MHz, CD_3CN) δ 1.20 (1H, m, *apex*), 1.23 (1H, m, *apex*), 2.75 (2H, d, *SCH*), 2.82 (2H, s, *bridgehead*), 6.29 (2H, t, *olefinic*). IR (KBr) 501, 497 ($\nu_{\text{Re}=\text{S}}$); 407 ($\nu_{\text{Re}=\text{S}}$).

$(\text{Ph}_4\text{P})_2[(\text{ReS}_2)_2(\text{S}_4\text{C}_7\text{H}_8)]$. A 100-mL Schlenk flask was charged with 0.47 g (0.71 mmol) of $\text{Ph}_4\text{P}[\text{ReS}_4]$, 50 mL of CH_3CN , and 0.039 mL (0.36 mmol) of 2,5-norbornadiene. After 3 h, the resulting yellow solution was concentrated to ~ 5 mL and diluted with 50 mL of Et_2O . The solvent was decanted, and the remaining solid was washed with Et_2O . Yield: 0.34 g (66%). This salt was not obtained in analytical purity but was further characterized by X-ray crystallography. ^1H NMR (500 MHz, CD_3CN) δ 1.22 (2H, m, *apex*), 2.63 (2H, t, *bridgehead*), 2.83 (2H, s, *SCH*). IR (KBr) 498, 491 ($\nu_{\text{Re}=\text{S}}$); 407 ($\nu_{\text{Re}=\text{S}}$).

General Procedure for UV–Vis Spectroscopy. Standardized solutions of $\text{Et}_4\text{N}[\text{ReS}_4]$ were prepared in volumetric flasks adapted for use on a Schlenk line. All solutions were prepared in the dark under a positive pressure of nitrogen. Solutions were then transferred via syringe into 10-mm glass cuvettes fitted with gas adapters and magnetic stir bars. Concentrated solutions of norbornene, norbornadiene, and dicyclopentadiene were prepared in volumetric flasks under nitrogen and were added to the reaction cuvette via microliter syringe. Ethylene was sparged through the ReS_4^- solution, and the reaction was maintained under a positive pressure (~ 1 atm) of ethylene. The optical spectrum of ReS_4^- in neat dimethyl maleate was obtained in air from the filtered solution.

Magnetization Transfer Experiments.⁵⁴ A solution of 5.0 mg (0.011 mmol) of $(\text{Et}_4\text{N})\mathbf{1}$ and 5.8 mg (0.062 mmol) of norbornene in ~ 7 mL of CD_3CN was flame-sealed into an NMR tube under vacuum. The intensity of the bound thiolato ipso CH signals decreased as the saturation time for the alkenyl H signal was extended. At the limit of long saturation times, the degree of magnetization was indicated by the intensity (I) vs the intensity in the absence of irradiation (I_0).

Electrochemistry. Voltammograms were recorded on a BAS 50W instrument, interfaced with a microcomputer. To 10 mL of 0.1 M $\text{Bu}_4\text{N}[\text{PF}_6]$ MeCN solution was added 0.0123 g (0.028 mmol) of $\text{Et}_4\text{N}[\text{ReS}_4]$ and 0.0421 g (0.45 mmol) of norbornene. The cyclic voltammogram of the resulting yellow solution was measured using a Pt working electrode, Pt wire for the common electrode, and aqueous Ag/AgCl as a reference.

Crystallographic Analysis of $\text{Ph}_4\text{P}[\text{ReS}_2(\text{S}_2\text{C}_7\text{H}_{10})]$. Gold prismatic crystals of $\text{Ph}_4\text{P}[\text{ReS}_2(\text{S}_2\text{C}_7\text{H}_{10})]$ were grown from MeCN solutions. The data crystal was attached to a thin glass fiber with Paratone-E oil (Exxon). The data crystal was bound by the (0 0–1), (0 1–1), (0 1 1), (1 0 1), and (1 0 0) faces. Distances from the crystal center to these

(54) Sanders, J. K. M.; Mersh, J. D. *Prog. Nucl. Magn. Reson. Spectrosc.* **1982**, *15*, 353–400.

Table 2. Crystallographic Data for $\text{Ph}_4\text{P}[\text{ReS}_2(\text{S}_2\text{C}_7\text{H}_{10})]$ and $(\text{Ph}_4\text{P})_2[(\text{ReS}_2)_2(\text{S}_4\text{C}_7\text{H}_8)]$

empirical formula	$\text{C}_{31}\text{H}_{30}\text{PReS}_4$	$\text{C}_{55}\text{H}_{48}\text{P}_2\text{Re}_2\text{S}_8$
formula weight	747.96	1399.75
space group	$P2_12_12_1$	$P1$
a , Å	10.4373(1)	12.6844(11)
b , Å	15.1269(2)	15.4061(5)
c , Å	18.6528(1)	16.000(2)
α , deg	90	62.200(7)
β , deg	90	83.795(6)
γ , deg	90	81.603(7)
V , Å ³	2944.98(5)	2733.3
Z	4	2
ρ_{calc} , g·cm ⁻³	1.687	1.701
absorption coefficient, mm ⁻¹	4.484	4.825
crystal size, mm	0.28 × 0.15 × 0.10	0.02 × 0.10 × 0.30
θ range, deg	1.73 to 28.25	1.44 to 22.50
reflections collected	19442 [$R(\text{int}) = 0.0797$]	11680 [$R(\text{int}) = 0.0549$]
independent reflections	7061 [5616 obs, $I > 2\sigma(I)$]	7059 [5196 obs, $I > 2\sigma(I)$]
$R1$ (obs data)	0.0285	0.0563
$wR2$ (obs data)	0.0540	0.1135
$R1$ (all data)	0.0431	0.0917
$wR2$ (all data)	0.0572	0.1448

facial boundaries were 0.050, 0.130, 0.140, 0.070, and 0.075 mm, respectively. Data were collected at 198 K on a Siemens CCD diffractometer.⁵⁵ Crystal and refinement details are given in Table 2. Systematic conditions suggested the space group $P2_12_12_1$. The structure was solved by Direct Methods;⁵⁶ correct positions for Re, S, P, and C were deduced from a vector-map. H atom U's were assigned as $1.2 \times U_{\text{eq}}$ of adjacent C atoms. Non-H atoms were refined with anisotropic thermal coefficients. Successful convergence of the full-matrix least-squares refinement of F^2 was indicated by the maximum shift/error of the last cycle.

Crystallographic Analysis of $(\text{Ph}_4\text{P})_2[(\text{ReS}_2)_2(\text{S}_4\text{C}_7\text{H}_8)]$. Gold plate-like crystals of $(\text{Ph}_4\text{P})_2[(\text{ReS}_2)_2(\text{S}_4\text{C}_7\text{H}_{10})_2]$ were grown from MeCN/Et₂O solutions. The data crystal was attached to a thin glass fiber with Paratone-E oil (Exxon). The data crystal was bound by the (0 0 -1), (0 -1 0), (1 0 0), and (1 2 1) faces. Distances from the crystal center to these facial boundaries were 0.010, 0.050, 0.150, and 0.080 mm, respectively. Data were collected at 198 K on a Siemens CCD diffrac-

tometer.⁵⁵ Crystal and refinement details are given in Table 2. Systematic conditions suggested the space group P . The structure was solved by Direct Methods;⁵⁶ correct positions for Re, S, and P were deduced from a vector map. Subsequent cycles of isotropic least-squares followed by an unweighted difference Fourier synthesis revealed positions for all C atoms. H atom U's were assigned as $1.2 \times U_{\text{eq}}$ of adjacent C atoms. Non-H atoms were refined with anisotropic thermal coefficients. Successful convergence of the full-matrix least-squares refinement of F^2 was indicated by the maximum shift/error of the last cycle.

Acknowledgment. This research was supported by the National Science Foundation. J.T.G. thanks the UIUC Department of Chemistry for a Drickamer Fellowship.

Supporting Information Available: Crystallographic data for the two structures including positional and thermal parameters, bond distances and angles (PDF). This material is available free of charge via the Internet at <http://pubs.acs.org>.

(55) Sheldrick, G. M. SAINT and SHELXTL, version 5, Bruker AXS, 1998.

(56) Sheldrick, G. M. SHELXL-97, University of Göttingen, 1997.